



Pathogenic Functions of Tumor Necrosis Factor Receptor-Associated Factor 6 Signaling Following Traumatic Brain Injury

Huan Huang^{1,2†}, Anqi Xia^{1,2†}, Li Sun^{1†}, Chun Lu³, Ying Liu⁴, Zhenjie Zhu¹, Siye Wang¹, Junyan Cai¹, Xiaoyun Zhou¹ and Su Liu^{1*}

¹ Department of Rehabilitation Medicine, Affiliated Hospital of Nantong University, Nantong, China, ² School of Medicine, Nantong University, Nantong, China, ³ Department of Rehabilitation Medicine, Shanghai General Hospital, Shanghai Jiao Tong University, Shanghai, China, ⁴ Department of Pathology, Affiliated Hospital of Nantong University, Nantong, China

OPEN ACCESS

Edited by:

Fabrizio Michetti,
Catholic University of the Sacred
Heart, Italy

Reviewed by:

Tiziano Balzano,
Centro Integral en Neurociencias A.C.
HM CINAC, Spain
Nadine Ahmed Kerr,
University of Miami, United States

*Correspondence:

Su Liu
327202278@qq.com

† These authors have contributed
equally to this work

Received: 16 November 2020

Accepted: 29 March 2021

Published: 21 April 2021

Citation:

Huang H, Xia A, Sun L, Lu C,
Liu Y, Zhu Z, Wang S, Cai J, Zhou X
and Liu S (2021) Pathogenic
Functions of Tumor Necrosis Factor
Receptor-Associated Factor 6
Signaling Following Traumatic Brain
Injury.
Front. Mol. Neurosci. 14:629910.
doi: 10.3389/fnmol.2021.629910

Neuroinflammation contributes to delayed (secondary) neurodegeneration following traumatic brain injury (TBI). Tumor necrosis factor receptor-associated factor 6 (TRAF6) signaling may promote post-TBI neuroinflammation, thereby exacerbating secondary injury. This study investigated the pathogenic functions of TRAF6 signaling following TBI *in vivo* and *in vitro*. A rat TBI model was established by air pressure contusion while lipopolysaccharide (LPS) exposure was used to induce inflammatory-like responses in cultured astrocytes. Model rats were examined for cell-specific expression of TRAF6, NF- κ B, phosphorylated (p)-NF- κ B, MAPKs (ERK, JNK, and p38), p-MAPKs, chemokines (CCL2 and CXCL1), and chemokine receptors (CCR2 and CXCR2) by immunofluorescence, RT-qPCR, western blotting, and ELISA, for apoptosis by TUNEL staining, and spatial cognition by Morris water maze testing. These measurements were compared between TBI model rats receiving intracerebral injections of TRAF6-targeted RNAi vector (AAV9-TRAF6-RNAi), empty vector, MAPK/NF- κ B inhibitors, or vehicle. Primary astrocytes were stimulated with LPS following TRAF6 siRNA or control transfection, and NF- κ B, MAPKs, chemokine, and chemokine receptor expression levels evaluated by western blotting and ELISA. TRAF6 was expressed mainly in astrocytes and neurons of injured cortex, peaking 3 days post-TBI. Knockdown by AAV9-TRAF6-RNAi improved spatial learning and memory, decreased TUNEL-positive cell number in injured cortex, and downregulated expression levels of p-NF- κ B, p-ERK, p-JNK, p-p38, CCL2, CCR2, CXCL1, and CXCR2 post-TBI. Inhibitors of NF- κ B, ERK, JNK, and p38 significantly suppressed CCL2, CCR2, CXCL1, and CXCR2 expression following TBI. Furthermore, TRAF6-siRNA inhibited LPS-induced NF- κ B, ERK, JNK, p38, CCL2, and CXCL1 upregulation in cultured astrocytes. Targeting TRAF6-MAPKs/NF- κ B-chemokine signaling pathways may provide a novel therapeutic approach for reducing post-TBI neuroinflammation and concomitant secondary injury.

Keywords: neuroinflammation, traumatic brain injury, rat model, lipopolysaccharide, TRAF6

INTRODUCTION

Severe traumatic brain injury (sTBI) is a frequent cause of physical disability, cognitive dysfunction, and accidental death. Physical and cognitive deficits result from both primary injury to the trauma site and delayed secondary injury to surrounding structures. Neuroinflammation is a major pathogenic mechanism for secondary brain injury following TBI (Chiu et al., 2016; Simon et al., 2017; Liu et al., 2019), characterized by edema, microglial and astrocytic activation and migration, and the release of inflammatory cytokines and chemokines (Gyoneva and Ransohoff, 2015; Karve et al., 2016; Webster et al., 2017). Thus, inhibition of these processes following sTBI may significantly reduce the progressive deficits associated with secondary brain injury.

Chemokines such as chemokine C-C motif ligand 2 (CCL2) and chemokine C-X-C motif ligand 1 (CXCL1) are critical signaling factors regulating post-TBI neuroinflammation. Cortical levels of these cytokines rise abruptly following injury, with CCL2 demonstrating higher peak levels compared to many other inflammatory mediators in TBI rats (Dalgard et al., 2012). Sustained elevation of CCL2 was detected in the cerebrospinal fluid (CSF) of sTBI patients for 10 days after trauma (Semple et al., 2010). Our preliminary study found that CCL2 was mainly co-localized with the astroglial marker glial fibrillary acidic protein (GFAP), while the CCL2 receptor chemokine C-C motif receptor 2 (CCR2) was mainly co-localized with the neuronal nuclear marker NeuN in TBI model rats, suggesting that CCL2–CCR2 signaling is a major driver of neuroinflammation, neurodegeneration, and concomitant motor and cognitive dysfunction following TBI (Liu et al., 2013a). We further demonstrated that *in vitro* administration of pro-inflammatory lipopolysaccharide (LPS) significantly upregulated expression levels of CCL2 and CXCL1 as well as phosphorylation (activation) of the stress-associated transcription factor nuclear factor-kappa B (NF- κ B) and the mitogen-activated protein kinases (MAPKs), c-jun N-terminal kinase (JNK), extracellular signal-regulated kinase (ERK), and p38 in cultured astrocytes prepared from cerebral cortices of neonatal rats. Conversely, neuroinflammation was modulated via regulation of LPS-induced MAPK/NF- κ B-CCL2/CXCL1 signaling pathways (Liu et al., 2018).

Tumor necrosis factor (TNF) receptor-associated factor 6 (TRAF6), a member of the TNF receptor-associated factor family, is a major regulator of central nervous system (CNS) development and neuroinflammation (Aarts et al., 2017; Li et al., 2017) as well as of neural cell apoptosis by directly

interacting with the death domain of caspase-8 (Dou et al., 2018). Chen et al. (2011) found that TRAF6 was highly expressed in cortical reactive astrocytes and neurons after TBI and promoted neuronal apoptosis. Other studies have reported that TRAF6 acts as an adaptor in a number of signaling pathways that positively regulate downstream kinase cascades, such as NF- κ B, JNK, and p-38, among others (Lu et al., 2014; Zeng et al., 2015; Li et al., 2019). Based on these findings, the present study examined if TRAF6 participates in severe TBI-induced neuroinflammation and associated functional deficits by regulating MAPK/NF- κ B-CCL2/CXCL1 signaling pathways. Further, we examined if disruption of these pathways or modulation of these signaling molecules expression can reduce neuroinflammation and functional deficits following severe TBI. Schematic of the possible mechanism of neuroinflammation following TBI is shown in **Figure 1**.

MATERIALS AND METHODS

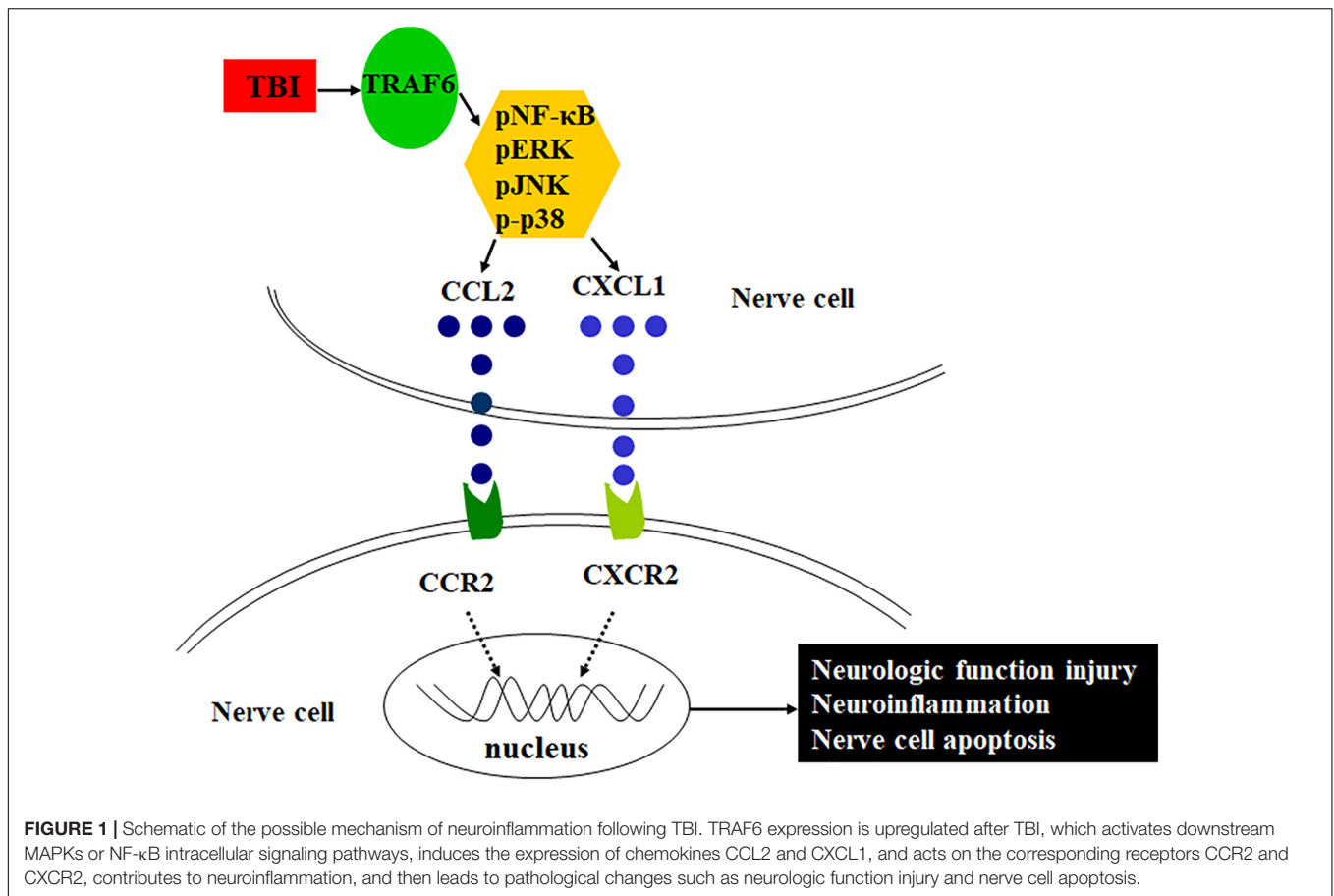
Animals and Surgery

Male Sprague–Dawley rats (230–270 g) were purchased from the Experimental Animal Center of Nantong University (Nantong, China) and housed in an animal room under controlled temperature ($23 \pm 2^\circ\text{C}$) and a 12-h/12-h light/dark cycle with free access to water and food; rats used for each experiment are shown in **Table 1**. All experimental procedures were approved by the Experimental Animal Ethics Committee of Nantong University. Severe traumatic brain injury was induced by controlled cortical impact (CCI) using air pressure (Xiong et al., 2013; Chiu et al., 2016), with slight modifications. Briefly, rats were anesthetized with 10% chloral hydrate, fixed in a stereotactic frame, and subjected to right parietal craniotomy with a dental drill (3 mm posterior to bregma, 3 mm from the midline, diameter of 6 mm) to expose the underlying dura mater. Injury was induced using the TBI-0310 impactor device (Precision Systems and Instrumentation, United States) with the following impact parameters: speed 4 m/s, depth 3 mm, and impact time 150 ms. After injury, the skull skin was sterilized with iodophor. The rat was then placed next to a heater until it regained consciousness before return to the home cage. A sham operation group underwent the same surgical procedure but did not receive experimental TBI.

Culture of Primary Cortical Astrocytes

Primary astrocyte cultures were prepared from the cerebral cortices of neonatal rats (Gao et al., 2009; Lu et al., 2014; Liu et al., 2018) purchased from the Experimental Animal Center of Nantong University. Bilateral cerebral cortices were isolated and transferred to ice-cold D-Hank's buffer. The meninges were carefully removed and the remaining tissues dissociated, filtered through nylon mesh (pore size of 100 μm), and collected by centrifugation at $\sim 3,000 \times g$ for 5 min. The cell pellet was dispersed with a pipette and resuspended in medium containing in low-glucose Dulbecco's Modified Eagle's Medium (DMEM, Life Technologies, Gibco BRL Division, Grand Island, NY, United States) supplemented with 10% fetal bovine serum (FBS).

Abbreviation: AAV, adeno-associated virus; AAV9, adeno-associated virus serotype 9; CCI, controlled cortical impact; CCL2, chemokine C-C motif ligand; CCR2, chemokine C-C motif receptor 2; CNS, central nervous system; CXCL1, chemokine (C-X-C motif) ligand 1; CXCR2, chemokine C-C motif receptor 2; DAPI, 4',6-diamidino-2-phenylindole; DMSO, dimethyl sulfoxide; ELISA, enzyme-linked immunosorbent assay; ERK, extracellular signal-regulated kinase; JNK, c-Jun N-terminal kinase; LPS, lipopolysaccharide; MAPKs, mitogen-activated protein kinases; NC, negative control; NF- κ B, nuclear factor-kappa B; siRNA, small interfering ribonucleic acid; sTBI, severe traumatic brain injury; TBI, traumatic brain injury; TRAF6, TNF receptor-associated factor 6; TUNEL, terminal deoxynucleotidyl transferase-mediated dUTP nick-end labeling.



The cells were then triturated using glass pipettes, filtered through a screen with 10- μ m pores, seeded on six-well plates at a density of 2.5×10^5 cells/cm², and cultured for approximately 10 days with medium replacement every 3 days. Dibutyryl cAMP sodium salt (0.15 mM; Sigma-Aldrich, St. Louis, MO, United States) was added to induce morphological and functional differentiation. The cells were used for experiments 3 days after reaching 90% confluence. Prior to experiments, the medium was replaced with Opti-MEM (Life Technologies, Inc-Gibco BRL Division). The cells were incubated with LPS (1 μ g/ml; Santa Cruz Biotechnology, Dallas, TX, United States) for 1–6 h and expression levels of inflammatory signaling factors measured by ELISA and western blotting as described below (Liu et al., 2018).

Adeno-Associated Virus Injection

We constructed an adeno-associated virus serotype 9 (AAV9) vector expressing TRAF6-specific RNAi (AAV9-TRAF6-RNAi) and an empty AAV9 vector (AAV-NC) (1.64×10^{13} v.g./ml) as a negative control according to the manufacturer's protocol (Jikai Gene, Shanghai, China). It was worth noting that AAV9-TRAF6-RNAi contained two specific promoters: the astrocyte promoter (1.36×10^{13} v.g./ml) and the neuronal promoter (1.22×10^{13} v.g./ml). So we mixed the two viruses with the astrocyte promoter and the neuronal promoter, respectively, in a ratio of 1:1. Male Sprague-Dawley rats (60–70 g) were randomly divided

into four groups: (1) sham, (2) TBI, (3) adeno-associated virus negative control (AAV9-NC) with TB, and (4) interference adeno-associated virus (AAV9-TRAF6-RNAi) with TBI. Rats were anesthetized by intraperitoneal injection of 10% chloral hydrate, shaved, sterilized, and fixed on a brain stereotaxic device. The forehead skin was cut along the midline and three holes drilled on the right side of the parietal bone with a dental drill (1.5 mm posterior to bregma, 1.5 mm lateral to the midline; 1.5 mm posterior to bregma, 3 mm lateral to the midline; 3 mm posterior to bregma, 1.5 mm lateral to the midline) through which 2 μ l of viral solution was injected per hole using Hamilton microliter syringes. Injection depth was 1.3 mm and injection speed was 0.2 μ l/min. The needle was kept in place for 8 min to insure full vector delivery. The TBI model was created as described 4 weeks after virus injection.

Drugs and Administration

Selective inhibitors of NF- κ B, ERK, JNK, and p38 were purchased from Calbiochem (Merck, Darmstadt, Germany) and dissolved in dimethyl sulfoxide (DMSO). One hour after TBI, the injured area was treated with NF- κ B inhibitor (BAY117082), ERK inhibitor (PD98059), JNK inhibitor (SP600125), or p38 inhibitor (SB203580) at 25 mg/10 ml (high dose) or 2.5 mg/10 ml (low dose) as indicated. Alternatively, corresponding control (vehicle) subgroups received 10 ml PBS+DMSO. All injections

were performed while the rat was fixed to a stereotaxic frame using 10 ml Hamilton microliter syringes. Drugs and solvent were injected at 2 ml/min (requiring about 5 min), and the needle was kept in place for 5 min. Rats received the indicated injections for three consecutive days. After TBI, the

surrounding damaged cerebral cortex tissue was collected for analysis of inflammatory factor expression levels by enzyme-linked immunosorbent assay (ELISA).

Astrocytes were transfected with a small interfering (si)RNA against TRAF6 (Guangzhou RiboBio Co., Ltd., Guangzhou, China) or negative control (NC) siRNA for 72 h and then stimulated with LPS. Afterward, the cells were collected for analysis by ELISA or western blotting.

TABLE 1 | Number of animals used for each experiment.

Experiment	Sham	TBI 1 day	TBI 3 days	TBI 7 days	TBI 10 days
Experiment 1					
Immuno fluorescence	3		3		
Experiment 2					
TRAF6+Western blot	3	3	3	3	3
Experiment 3					
AAV9-TRAF6-RNAi+MWM			10		
AAV9-TRAF6-NC+MWM			10		
MWM	10		10		
Experiment 4					
AAV9-TRAF6-RNAi+TUNEL			3		
AAV9-TRAF6-NC+TUNEL			3		
TUNEL	3		3		
Experiment 5					
AAV9-TRAF6-RNAi+Western blot			3		
AAV9-TRAF6-NC+Western blot			3		
Western blot	3		3		
Experiment 6					
AAV9-TRAF6-RNAi+RT-PCR/ELISA			6		
AAV9-TRAF6-NC+RT-PCR/ELISA			6		
RT-PCR/ ELISA	6		6		
Experiment 7					
High-dose BAY117082+ ELISA			6		
Low-dose BAY117082+ ELISA			6		
High-dose PD98059+ ELISA			6		
Low-dose PD98059+ ELISA			6		
High-dose SP600125+ ELISA			6		
Low-dose SP600125+ ELISA			6		
High-dose SB203580+ ELISA			6		
Low-dose SB203580+ ELISA			6		
ELISA	6		6		

Immunofluorescence

Rats were anesthetized by intraperitoneal injection of 10% chloral hydrate, perfused through the heart with normal saline until the liver became white, and then perfused with 4% paraformaldehyde. The whole brain was post-fixed overnight in 4% paraformaldehyde, dehydrated in 20 and 30% sucrose solutions, and then coronally cryo-sectioned to 20- μ m slices. The slices were first blocked with 1% bovine serum albumin (BSA) for 2 h at room temperature and incubated overnight at 4°C with mouse anti-TRAF6 monoclonal antibody (sc-8409, 1:200, Santa Cruz Biotechnology) plus the astrocyte marker rabbit anti-GFAP monoclonal antibody (ab7260, 1:500, abcam), the microglial marker goat anti-IBA-1 monoclonal antibody (ab5076, 1:500, abcam), or the neuronal marker rabbit anti-NeuN monoclonal antibody (ab177487, 1:500, abcam). Slices were then incubated at room temperature with Cy3-conjugated and Alexa 488-conjugated secondary antibodies (1:1000, Jackson ImmunoResearch, West Grove, PA, United States) for 2 h. The stained sections were examined with a Nikon Ni-E microscope at 20 \times magnification. Images were analyzed by ImageJ software (NIH).

Morris Water Maze Test

Three days before TBI modeling, the rats received successive adaptive training trials in the Morris water maze to eliminate the influences of vision and motor function on performance. Place navigation learning was tested starting on the third day after TBI, and the spatial probe trial for spatial memory was conducted 24 h later (Liu et al., 2013b; Tucker et al., 2018). Escape latency to the platform was measured on each of four daily learning trials and averaged. We also recorded swim paths during each trial. If the rat did not reach the platform within 120 s, it was guided to the platform and allowed to stay for 30 s. The escape latency in such cases was recorded as 120 s. The probe trial examined spatial memory for the original platform location by recording the number of crossings over the former platform location after release from the quadrant opposite the target quadrant. Two probe trials were conducted and the average recorded for analysis.

TUNEL

Terminal deoxynucleotidyl transferase-mediated dUTP nick-end labeling (TUNEL) staining was performed to detect DNA fragmentation as an index of programmed cell death in brain tissues using an apoptosis detection kit (A113, Vazyme, Nanjing, China) according to the manufacturer's protocol. The red fluorescence of fluorescein-12-dUTP was detected against the blue background of 4',6-diamidino-2-phenylindole (DAPI) under a fluorescence microscope at 20 \times magnification. The

TUNEL-positive cells in the injured cortex were identified and counted by ImageJ software (NIH).

Real-Time Quantitative Polymerase Chain Reaction

Rats were anesthetized with 10% chloral hydrate and then perfused via the heart with PBS until the liver turned white. The cerebral cortex around the injured area was excised and total RNA extracted using TRIzol. The RNAs were then reversed transcribed to cDNA. Real-time PCR was performed in a Step One Plus real-time qPCR instrument using the primer sequences shown in **Table 2** and the following PCR amplification conditions: pre-denaturation at 95°C for 3 min; 40 cycles of 95°C for 10 s and 60°C for 30 s; dissolution at 95°C for 15 s, 60°C for 60 s, and 95°C for 15 s. Expression of GAPDH served as the internal control and gene expression level was determined using the $2^{-\Delta \Delta CT}$ method.

Western Blot

Western blotting was performed according to the previous study (Liu et al., 2018). The antibodies used were shown as follows: TRAF6 (sc-8409,1:500, Santa Cruz), p-NF- κ B (3033, 1:1000, Cell Signaling, Danvers, MA, United States), p-ERK (9101, 1:1000, Cell Signaling), p-JNK (4688,1:1000, Cell Signaling), p-p38 (9211,1:1000, Cell Signaling), and GAPDH (MAB374,1:10,000, Millipore, Billerica, MA, United States).

ELISA

Cell proteins were prepared as described for western blotting and added at 100 μ g/well to 96-well plates prepared for ELISA according to the kit manufacturers' instructions (below). The absorbance of each well at 450 nm was measured and target protein concentrations calculated according to standard curves prepared by the dilution of standards. A rat CXCL1 ELISA kit was purchased from Hangzhou MultiSciences (Lianke) Biotech (EK396/2-96, Hangzhou, Zhejiang, China), a rat CCL2 ELISA kit from R&D Systems (MJE00, Minneapolis, MN, United States), a rat CCR2 ELISA kit from CUSABIO TECHNOLOGY (CSB-EL004841RA, Wuhan, Hubei, China), and a rat CXCR2 ELISA kit from Cloud-Clone Corp (SEC006Ra, Katy, TX, United States).

TABLE 2 | Primer sequences.

Genes	Primers	Sequences (5'–3')
GAPDH	Forward	TCCTACCCCAATGTATCCG
	Reverse	CCTTTAGTGGGCCCTCGG
CCL2	Forward	TGCTGCTACTCATTCACTGGC
	Reverse	CCTTATTGGGGTCAGCACAG
CCR2	Forward	TGCTACTCAGGAATCCTCCACAC
	Reverse	GGCCTGGTCTAAGTGCATGTCAAC
CXCL1	Forward	GCACCCAAACCGAAGTCATA
	Reverse	GGGGACACCCCTTAGCATCT
CXCR2	Forward	TGGTCCTCGTCTTCTGCTCTG
	Reverse	CGTTCTGGCGTTCACAGGTCTC

Statistical Analysis

All measurement data are expressed as mean \pm SEM. Multiple group means were compared by one-way ANOVA with post hoc Bonferroni correction. A $P < 0.05$ (two-tailed) was considered significant for all tests. All statistical analyses were conducted using GraphPad Prism 5.0 (San Diego, CA, United States).

RESULTS

Co-localization of TRAF6 With Neuron and Astrocyte Markers in Cerebral Cortex of Traumatic Brain Injury (TBI) Model Rats

To determine the specific cell types expressing TRAF6, we performed double immunofluorescence staining using anti-TRAF6 and a second cell-specific marker (GFAP, NeuN, or IBA-1). TRAF6 mainly co-localized with the astrocyte marker GFAP (**Figures 2A–C**) and the neuronal marker NeuN (**Figures 2D–F**) but demonstrated almost no co-localization with the microglial marker IBA-1 (**Figures 2G–I**). According to manual cell counting, $55 \pm 3\%$ of astrocytes, $39 \pm 2\%$ of neurons, and $6 \pm 1\%$ of microglia expressed detectable TRAF6 (**Figure 2J**).

TBI Induced Region-Specific Upregulation of TRAF6 Expression in Cerebral Cortex

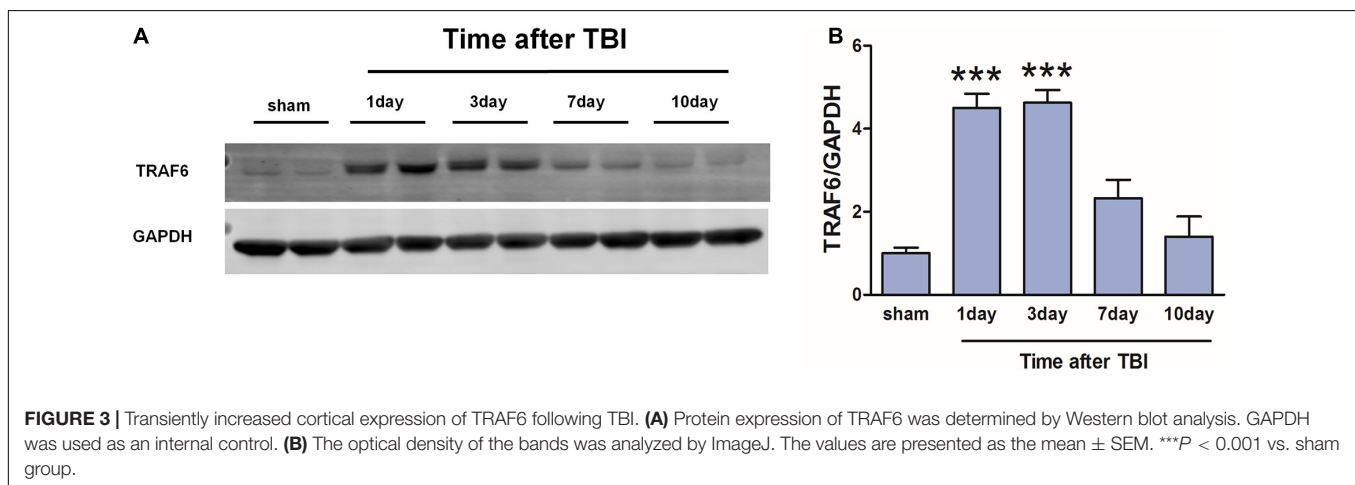
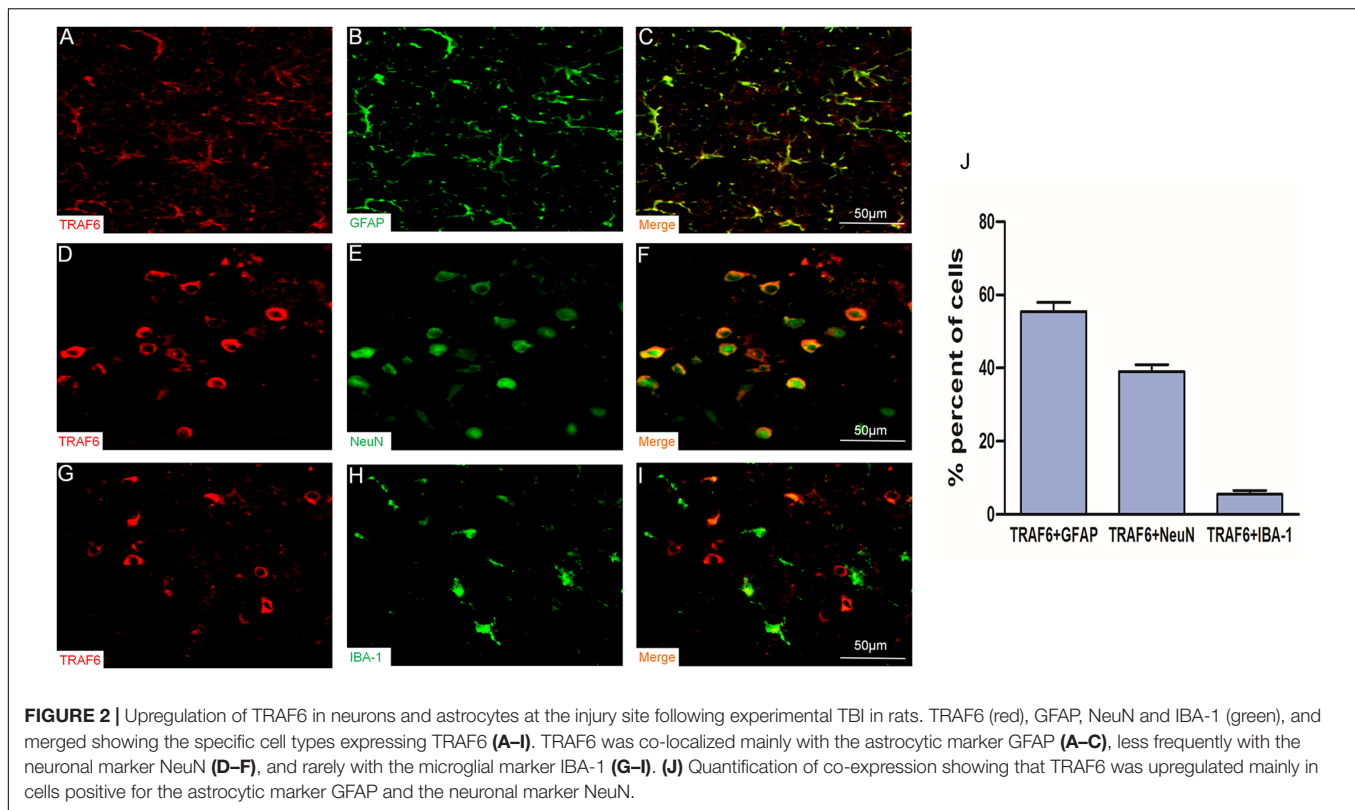
Western blot was used to detect changes in cortical TRAF6 expression at 1, 3, 7, and 10 days post-TBI (**Figure 3**). On day 1 post-TBI, TRAF6 expression was significantly greater in the injured area of the TBI group compared to the sham group. Expression reached a peak at 3 days post-TBI and then gradually declined.

AAV9-TRAF6-RNAi Injection Rescued Spatial Cognition

To evaluate whether TRAF6 signaling pathways contribute to cognitive dysfunction after TBI, rat subgroups receiving Sham, TBI, AAV9-NC+TBI, or AAV9-TRAF6-RNAi+TBI were compared for spatial learning and memory in the Morris water maze. Cognitive functions were significantly decreased after brain injury in the TBI group which compared with sham group. The average latency to the hidden platform during learning trials was significantly lower in the AAV9-TRAF6-RNAi+TBI group compared to TBI and AAV9-NC+TBI groups (**Figure 4A**), while in the probe trial, the mean number of platform location crossing was significantly greater in the AAV9-TRAF6-RNAi group (**Figure 4B**). Thus, suppression of the post-TBI increase in TRAF6 partially rescued spatial learning and memory.

AAV9-TRAF6-RNAi Injection Reduced Nerve Cell Neuronal Apoptosis After TBI

We used TUNEL staining of cortical sections to examine the effect of TBI-induced TRAF6 signaling on apoptosis, a major cell death pathway contributing to secondary injury. The number



of TUNEL positive (apoptotic) cells was significantly higher in the TBI group compared to that of the sham group. Cell counting revealed a significant decrease in TUNEL-positive cells 3 days post-TBI in TBI model rats receiving AAV9-TRAF6-RNAi compared to the AAV9-NC-treated TBI group (Figure 5).

AAV9-TRAF6-RNAi Downregulated the Expression Levels of p-NF- κ B, p-ERK, p-JNK, and p-p38 in Injured Cortex

Based on the above results and our previous research (Lu et al., 2014; Liu et al., 2018), we speculated that p-NF- κ B,

p-ERK, p-JNK, and p-p38 may be TRAF6-activated downstream signaling factors contributing to secondary degeneration following TBI. To test this hypothesis, we compared the expression changes in p-NF- κ B, p-ERK, p-JNK, and p-p38 among TBI model rats receiving AAV9-TRAF6-RNAi or AAV9-NC pretreatment. Consistent with activation of these signaling pathways by TRAF6, the results showed that the TBI increased the production of p-NF- κ B, p-ERK, p-JNK, and p-p38 compared to the sham group, the expression levels of p-NF- κ B, p-ERK, p-JNK, and p-p38 at the site of injury were significantly lower in the AAV9-TRAF6-RNAi+TBI group compared to the AAV9-NC+TBI group on day 3 post-TBI (Figure 6).

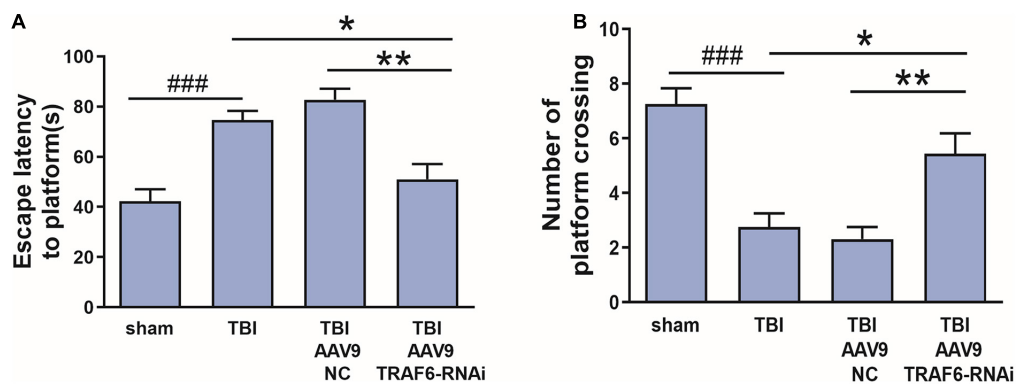


FIGURE 4 | Knockdown of TRAF6 after TBI rescued spatial learning and memory. Sham and TBI model rats receiving intracerebral injection of knockdown vector (AAV9-TRAF6-RNAi) or negative control vector (AAV9-NC) were compared for spatial learning and memory in the Morris water maze at 3 days post-TBI (or sham surgery). **(A)** Escape latency is presented as mean \pm SEM (s). Administration of AAV9-TRAF6-RNAi reduced average latency to the escape platform, indicating improved spatial learning following TBI. * $P < 0.05$ and ** $P < 0.01$ vs. AAV9-TRAF6-RNAi group. ### $P < 0.001$ vs. sham group. **(B)** The number of platform location crossings is presented as mean \pm SEM. Administration of AAV9-TRAF6-RNAi increased the number of platform crossings following TBI, indicating improved spatial memory. * $P < 0.05$ and ** $P < 0.01$ vs. AAV9-TRAF6-RNAi group. ### $P < 0.001$ vs. sham group.

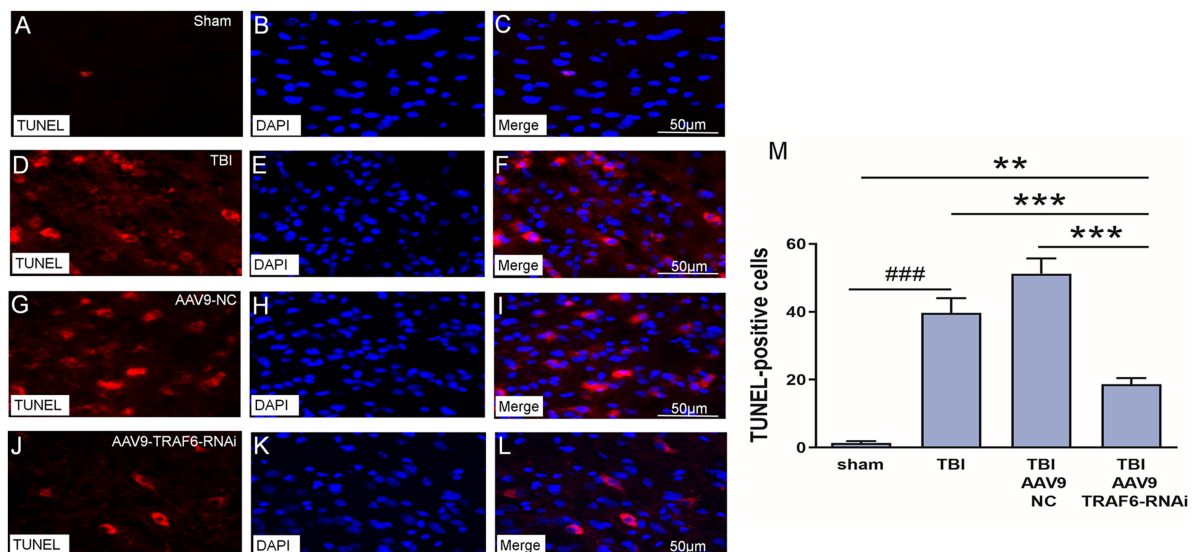


FIGURE 5 | Knockdown of TRAF6 reduced apoptotic death rate following TBI. TUNEL (red), DAPI (blue), and TUNEL+DAPI (merged) images showing apoptotic nerve cell. **(A–C)** Sham-treated rats. **(D–F)** TBI model rats. **(G–I)** TBI model rats injected with AAV9-NC. **(J–L)** TBI model rats injected with AAV9-TRAF6-RNAi. Scale bars are equal to 50 μ m. **(M)** AAV9-TRAF6-RNAi treatment decreased nerve cell apoptosis. Values are presented as mean \pm SEM. ** $P < 0.01$ and *** $P < 0.001$ vs. AAV9-TRAF6-RNAi group. ### $P < 0.001$ vs. sham group.

AAV9-TRAF6-RNAi Downregulated mRNA and Protein Expression Levels of CCL2, CCR2, CXCL1, and CXCR2 in Injured Cortex

We also speculated that CCL2 and CXCL1 may be downstream effectors of TRAF6-MAPK-NF- κ B signaling. To test this hypothesis, we compared mRNA and protein expression levels of CCL2, CXCL1, CCR2, and CXCR2 between TBI model rats receiving AAV9-TRAF6-RNAi or AAV9-NC pretreatment (Figure 7). Indeed, consistent with regulation by TRAF6, AAV9-TRAF6-RNAi

downregulate the mRNA expression levels (Figures 7A–D) and protein expression levels (Figures 7E–H) of CCL2, CCR2, CXCL1, and CXCR2, which had been induced by TBI for 3 days.

NF- κ B, ERK, JNK, and p38 Inhibitors Also Reduced Protein Expression Levels of CCL2, CCR2, CXCL1, and CXCR2 in Injured Cortex

In our previous study (Liu et al., 2018), we demonstrated that NF- κ B, ERK, and JNK inhibitors reduced CCL2 and

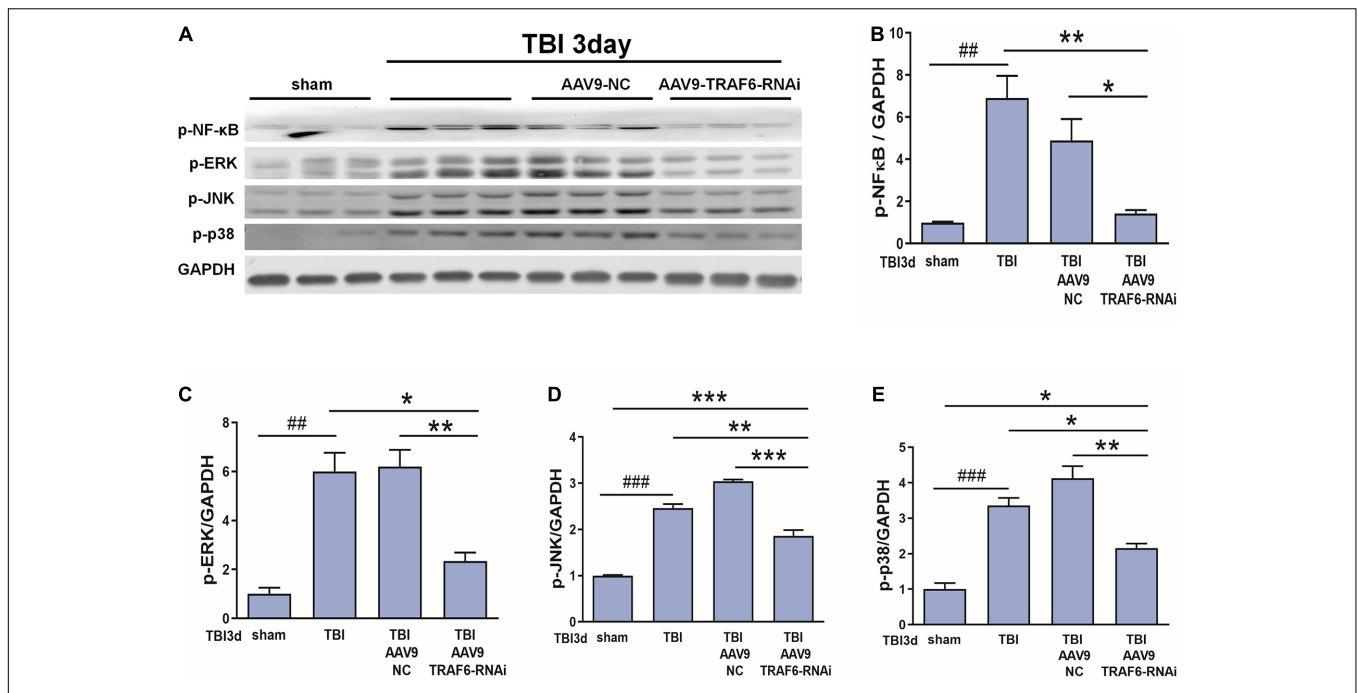


FIGURE 6 | TRAF6 knockdown reduced p-NF-κB, p-ERK, p-JNK, and p-p38 expression in the injured cortex after TBI. **(A)** Western blot analysis was used to detect the expression of p-NF-κB, p-ERK, p-JNK, and p-p38. GAPDH was used as an internal control. **(B–E)** The optical density of the bands was analyzed by ImageJ. **P* < 0.05, ***P* < 0.01, and ****P* < 0.001 vs. AAV9-TRAF6-RNAi group. ##*P* < 0.01 and ###*P* < 0.001 vs. sham group.

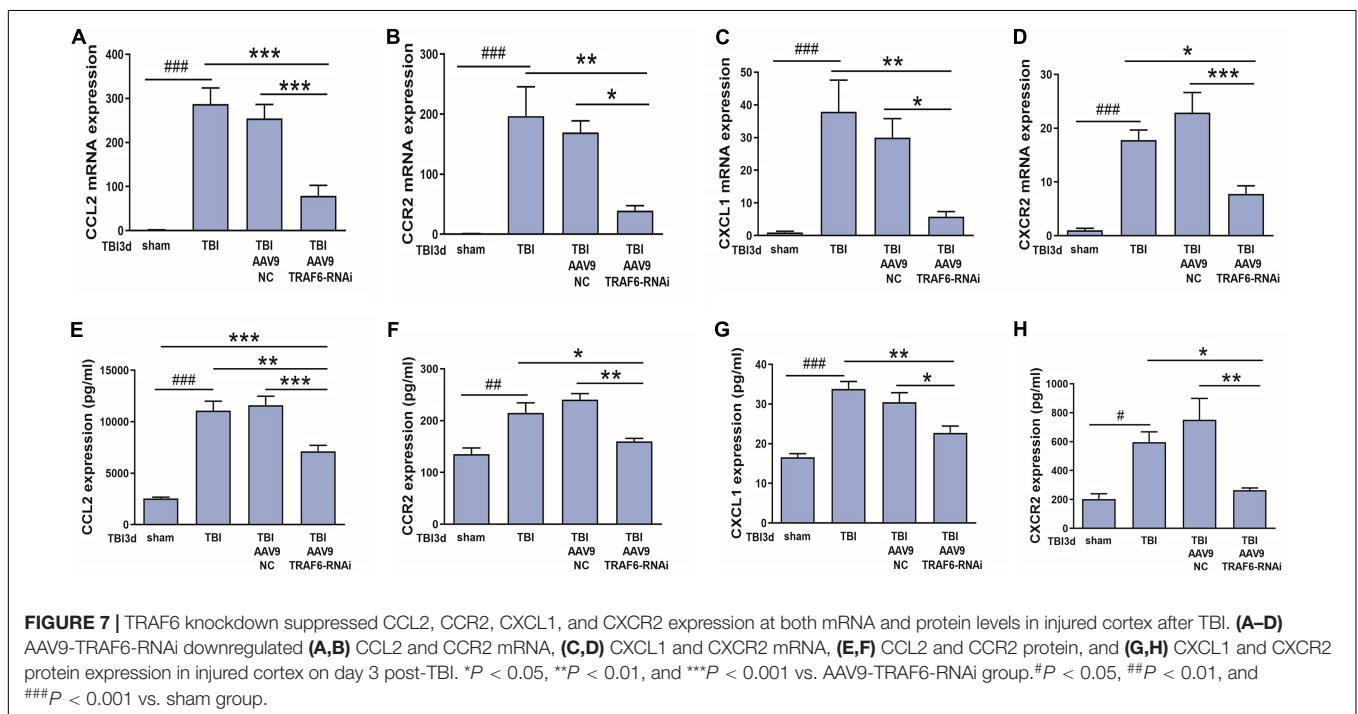
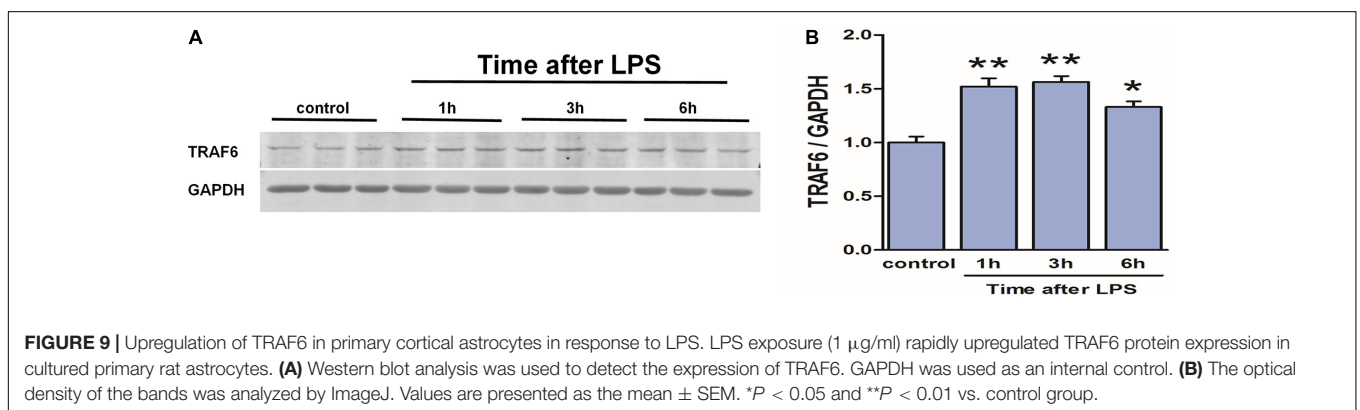
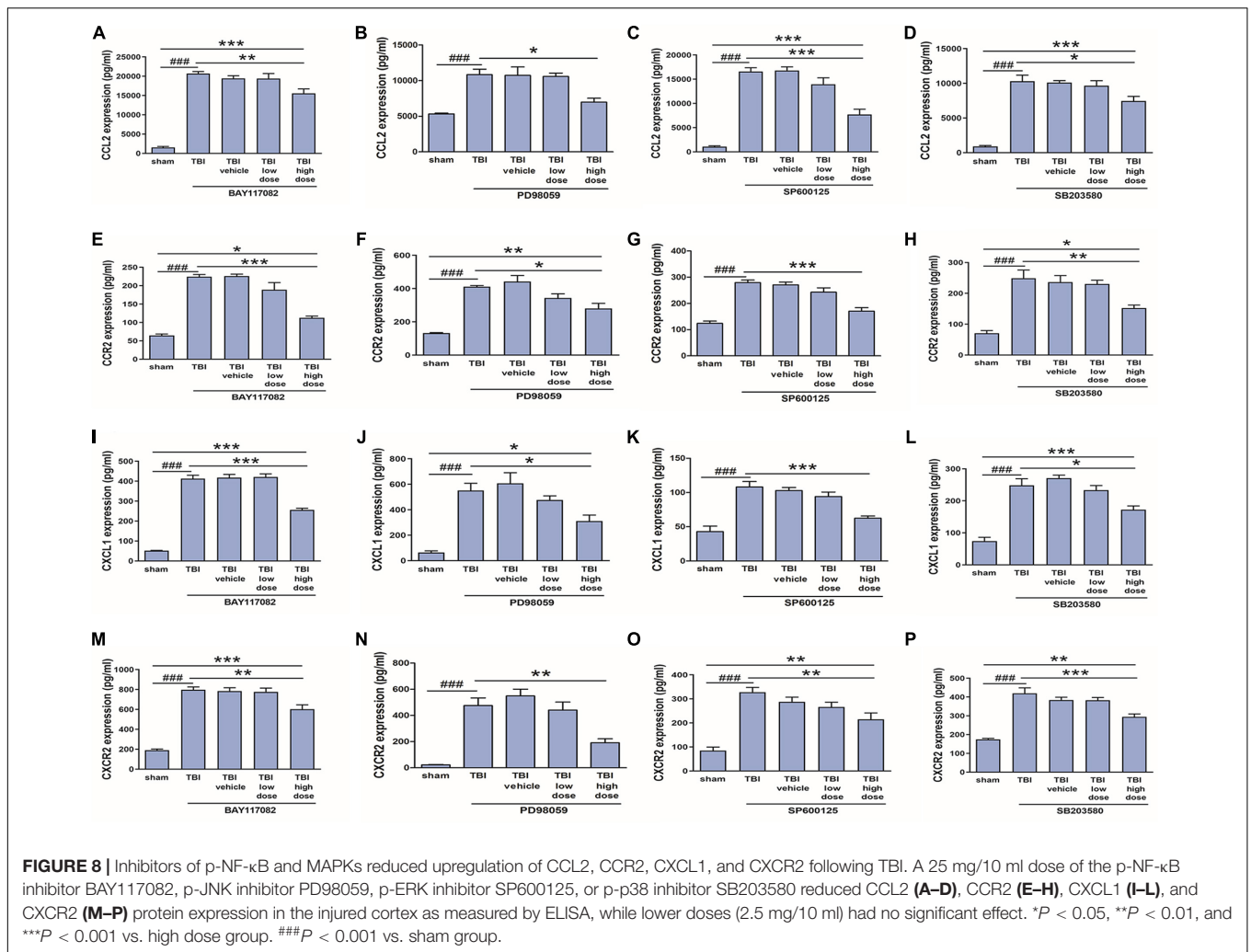


FIGURE 7 | TRAF6 knockdown suppressed CCL2, CCR2, CXCL1, and CXCR2 expression at both mRNA and protein levels in injured cortex after TBI. **(A–D)** AAV9-TRAF6-RNAi downregulated **(A,B)** CCL2 and CCR2 mRNA, **(C,D)** CXCL1 and CXCR2 mRNA, **(E,F)** CCL2 and CCR2 protein, and **(G,H)** CXCL1 and CXCR2 protein expression in injured cortex on day 3 post-TBI. **P* < 0.05, ***P* < 0.01, and ****P* < 0.001 vs. AAV9-TRAF6-RNAi group. #*P* < 0.05, ##*P* < 0.01, and ###*P* < 0.001 vs. sham group.

CXCL1 expression in activated astrocytes. To verify these effects *in vivo*, we measured changes in CCL2, CXCL1, CCR2, and CXCR2 protein expression levels among model rats treated with low (2.5 mg/10 ml) or high (25 mg/10 ml) doses of NF-κB, ERK, JNK, and p38 inhibitors. Indeed, a high dose of

the NF-κB inhibitor BAY117082, ERK inhibitor PD98059, JNK inhibitor SP600125, or p38 inhibitor SB203580 downregulates expression of CCL2, CCR2, CXCL1, and CXCR2 at the protein level (**Figures 8A–P**), which had been induced by TBI for 3 days. Thus, TRAF6-MAPK/NF-κB signaling pathways

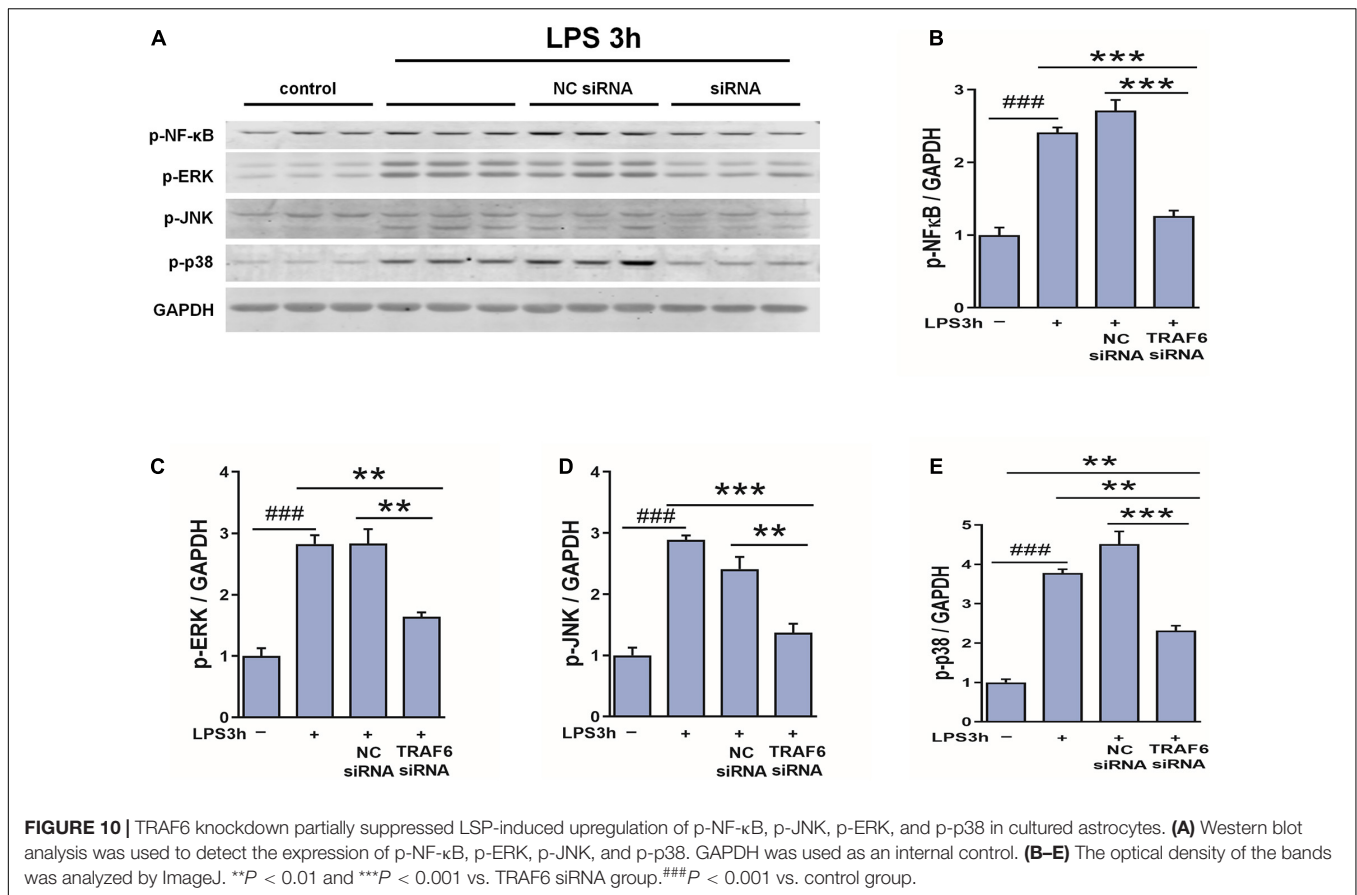


appear to mediate upregulation of CCL2, CCR2, CXCL1, and CXCR2 following TBI.

LPS Induced TRAF6 Upregulation in Cultured Astrocytes

To verify the link between neuroinflammation and TRAF6 upregulation in astrocytes (the predominant cell type showing

TRAF6 upregulation after TBI, **Figure 2**), we measured TRAF6 protein expression changes in primary astrocytes at 1, 3, and 6 h following stimulation (activation) by the inflammatory inducer LPS (**Figure 9**). Expression levels of TRAF6 in primary astrocytes were higher at 1 h post-LPS compared to the sham-treated control group and peaked at 3 h before gradually decreasing.



TRAF6 Knockdown Suppressed p-NF- κ B, p-JNK, p-ERK, and p-p38 Expression in LPS-Treated Cultured Astrocytes

To examine if TRAF6 upregulation in astrocytes activates NF- κ B, JNK, ERK, and p38 as downstream effectors, we compared LPS-induced changes in the expression levels of the phosphorylated forms between control astrocytes and astrocytes transfected with TRAF6 siRNA (Figure 10). Indeed, TRAF6 siRNA significantly suppressed LPS-induced upregulation of p-NF- κ B, p-JNK, p-ERK, and p-p38 at 3 h post-stimulation. Collectively, these findings (Figures 9, 10) suggest that MAPK/NF- κ B signaling pathways are induced in activated astrocytes at the site of TBI via upregulation of TRAF6.

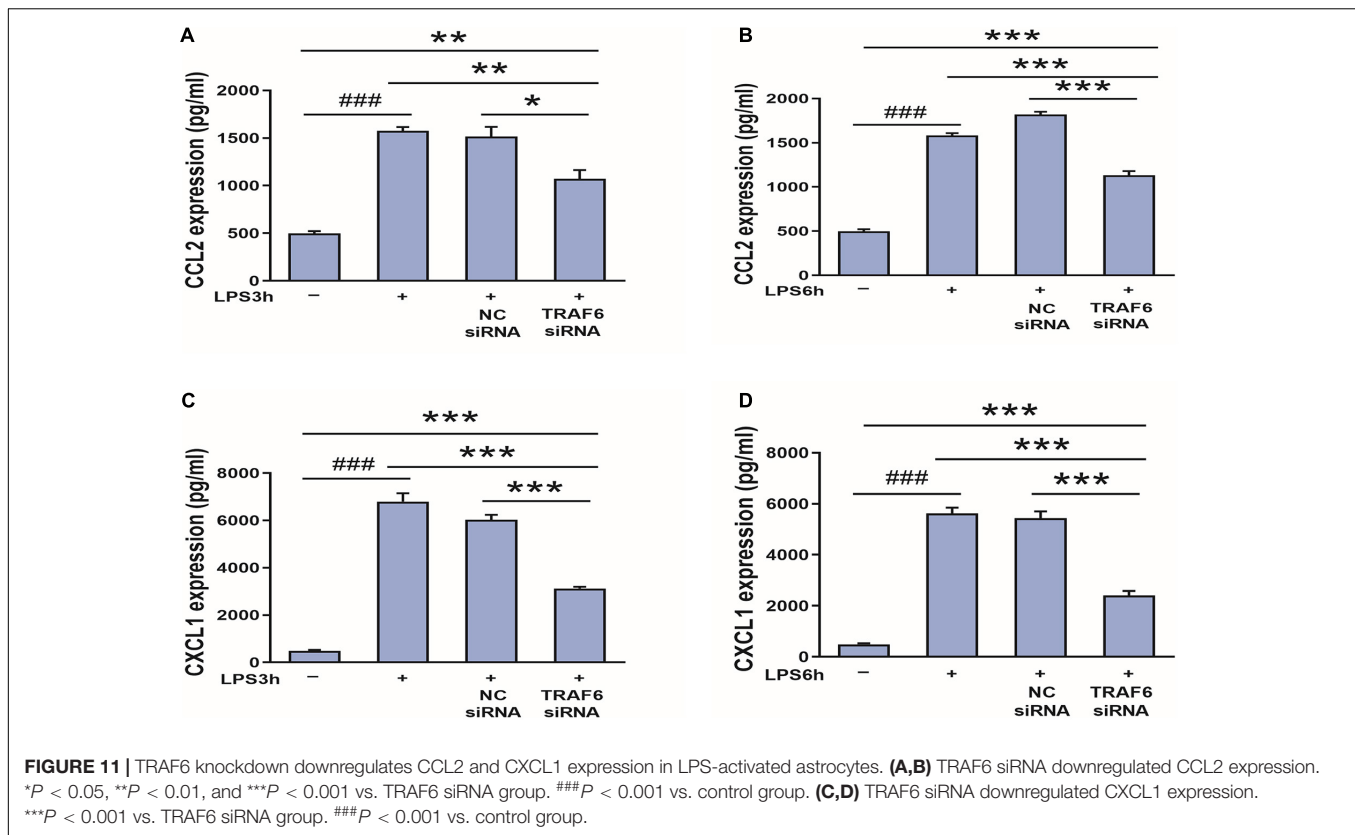
TRAF6 Knockdown Suppressed CCL2 and CXCL1 Expression in LPS-Treated Astrocytes

Finally, to examine if CCL2 and CXCL1 are downstream effectors of TRAF6, expression levels were compared between control astrocyte cultures and cultures pretreated with TRAF6 siRNA. As shown in Figure 11, TRAF6 siRNA significantly reduced CCL2 and CXCL1 expression levels in astrocytes treated for 3 or 6 h with LPS treatment.

DISCUSSION

Tumor necrosis factor receptor-associated factor 6 acts as a critical regulator of acquired immunity by binding to TNF super family and Toll/interleukin-1 receptor super family members. Due to the large number of binding partners, TRAF6 can exert complex regulation of inflammatory signaling pathways. Numerous studies have reported TRAF6 upregulation associated with CNS damage due to TBI, stroke, neurodegenerative diseases, and neuropathies (Chen et al., 2011, 2019; Aarts et al., 2017; Dou et al., 2018; Wu et al., 2018). In the present study, we found that TRAF6 was mainly expressed in astrocytes and neurons of injured cortex and that the expression level of TRAF6 reached its peak in the injured cerebral cortex 3 days following experimental TBI. TRAF6 knockdown also reduced neuronal apoptosis and rescued spatial learning and memory at 3 days after TBI. Therefore, TRAF6 may play an important role in secondary neuroinflammatory injury in the early stages after TBI.

Traumatic brain injury in rats significantly upregulated the local expression levels of NF- κ B, MAPKs (ERK, JNK, and p38), and other signaling molecules implicated in the neuroinflammatory response of rats following TBI (Chu et al., 2013; Kim et al., 2015; Marshall et al., 2017; Yang et al., 2017). Suppression of these inflammatory signaling pathways may thus reduce secondary injury from TBI (Geng et al., 2016; Meng et al., 2016; Qian et al., 2017; Kong et al., 2019).



In this study, we used AAV9-TRAF6-RNAi to interfere with the expression of TRAF6 and found that knockdown significantly reduced the upregulation of p-NF- κ B, p-JNK, p-ERK, p-p38, CCL2, CCR2, CXCL1, and CXCR2 expression levels observed after TBI, indicating that TRAF6 could regulate these signal molecules. We further found that application of inhibitors of NF- κ B, p38, ERK, and JNK decreased the upregulated expression of CCL2, CCR2, CXCL1, and CXCR2 following TBI, showing that NF- κ B, p38, ERK, and JNK could regulate CCL2, CCR2, CXCL1, and CXCR2. Collectively, these results indicate that TRAF6 upregulation in astrocytes and neurons after TBI induces neurologic dysfunction and apoptosis by activating NF- κ B/MAPK-CCL2/CXCL1 signaling pathways, while AAV9-TRAF6-RNAi likely alleviated post-TBI neuroinflammation by targeting NF- κ B/ ERK/JNK/p38-CCL2/CXCL1 signaling pathways.

Astrocytes and microglia are the major immune cells of the brain parenchyma that mediate inflammation. We had verified that downstream signal molecule of TRAF6 including CCL2 and CXCL1 was mainly expressed in astrocytes of injured cortex after TBI in our previous study *in vivo*. Our previous study further showed that LPS significantly upregulated CCL2, CXCL1, p-NF- κ B, p-ERK, p-JNK, and p-p38 in cultured astrocytes *in vitro*, and that inhibitors of NF- κ B, ERK, and JNK partially suppressed CCL2 and CXCL1 overexpression induced by LPS. Alternatively, the p38 inhibitor had no obvious effect on expression levels of CCL2 and CXCL1. We further demonstrated that reducing neuroinflammation via

downregulation of LPS-induced MAPKs (ERK and JNK)/NF- κ B-CCL2/CXCL1 signaling pathways in astrocytes (Liu et al., 2018). Results of the study indicated that LPS induced significant upregulation of TRAF6 in primary cultured astrocytes and the peak expression level was reached after 3 h of LPS treatment. Based on our preliminary data, astrocytes were transfected with a small interfering siRNA against TRAF6 in this study. We found that a TRAF6 siRNA downregulated the expression levels of CCL2, CXCL1, p-NF- κ B, p-ERK, p-JNK, and p-p38 in cultured astrocytes activated by LPS. Taken together, these results suggest that TRAF6 can modulate neuroinflammation via regulation of the LPS-induced-MAPKs (ERK and JNK)/NF- κ B-CCL2/CXCL1 signaling pathways in cultured astrocytes, while additional studies are needed to delineate the contribution of p38 signaling pathways. TRAF6 partly expressed in microglia ($6 \pm 1\%$) except astrocytes and neurons in the study. TRAF6 is an important adaptor of the TLR4/MAPK/NF- κ B signaling pathway that could induce p38/JNK phosphorylation in LPS-activated BV2 microglia cells, and TRAF6-JNK/p38-ATF2 axis might promote microglial inflammatory activation and thus aggravate neuronal injury in brain (Li et al., 2019). Inhibiting the TRAF6-related signaling pathways by alleviating microglia-mediated neuroinflammation injury could exert anti-inflammatory and neuroprotective effects (Song et al., 2016). We will establish an astrocyte-neuron co-culture and microglia-neuron co-culture to explore the role of TRAF6 signaling pathways between astrocytes/microglia and neurons in the next experiment.

TRAF6 signaling pathways mediate neuroinflammation in many diseases, so modulation of these inflammatory pathways may be a broadly effective treatment strategy. For instance, recombinant growth-arrest-specific protein 6 reduced neuroinflammation after middle cerebral artery occlusion in rats by disrupting TLR-TRAF-NF- κ B signaling at the level of TRAF6 (Wu et al., 2018), and a small molecule inhibitor of CD40-TRAF6 signaling was shown to reduce inflammation in rodent models of multiple sclerosis (Aarts et al., 2017). Neuroinflammation was alleviated by blocking of the TRAF6/NLRP3 interaction during intracerebral hemorrhage that may shed new light on intracerebral hemorrhage treatment in clinic (Wan et al., 2021). Zinc finger protein A20 suppressed the inflammatory response following intracerebral hemorrhage by regulating TRAF6 polyubiquitination (Meng et al., 2017). MiR-146a was involved in the regulation of brain inflammation by modulating TRAF6/NF- κ B or MAPK signaling pathways and could be considered a novel therapeutic agent for treating brain inflammation (Liu et al., 2020). We demonstrate that TRAF6 knockdown partially suppressed multiple inflammatory signaling pathways, reduced nerve cell apoptosis, and improved cognitive function following TBI. Therefore, further studies are warranted to explore potential therapies based on the inhibition of TRAF6-MAPKs (ERK and JNK)/NF- κ B-CCL2/CXCL1 signaling following TBI.

CONCLUSION

Our study demonstrates that TRAF6-MAPKs/NF- κ B-CCL2/CXCL1 signaling pathways possibly mediate neuroinflammation following TBI, which in turn leads to neurodegeneration and cognitive dysfunction. Targeting these signaling pathways may provide a novel therapeutic approach for the treatment of secondary injury after TBI.

REFERENCES

- Aarts, S., Seijkens, T. T. P., Kusters, P. J. H., van der Pol, S. M. A., Zarzycka, B., Heijnen, P., et al. (2017). Inhibition of cd40-traf6 interactions by the small molecule inhibitor 6877002 reduces neuroinflammation. *J. Neuroinflammation* 14:105. doi: 10.1186/s12974-017-0875-9
- Chen, J., Wu, X., Shao, B., Zhao, W., Shi, W., Zhang, S., et al. (2011). Increased expression of tnfr receptor-associated factor 6 after rat traumatic brain injury. *Cell. Mol. Neurobiol.* 31, 269–275. doi: 10.1007/s10571-010-9617-6
- Chen, L., Kong, L., Wei, X., Wang, Y., Wang, B., Zhang, X., et al. (2019). Beta-arrestin 2 negatively regulates nod2 signalling pathway through association with traf6 in microglia after cerebral ischaemia/reperfusion injury. *J. Cell. Mol. Med.* 23, 3325–3335. doi: 10.1111/jcmm.14223
- Chiu, C. C., Liao, Y. E., Yang, L. Y., Wang, J. Y., Tweedie, D., Karnati, H. K., et al. (2016). Neuroinflammation in animal models of traumatic brain injury. *J. Neurosci. Methods* 272, 38–49. doi: 10.1016/j.jneumeth.2016.06.018
- Chu, W., Li, M., Li, F., Hu, R., Chen, Z., Lin, J., et al. (2013). Immediate splenectomy down-regulates the mapk-nf-kappab signaling pathway in rat brain after severe traumatic brain injury. *J. Trauma Acute Care Surg.* 74, 1446–1453. doi: 10.1097/TA.0b013e31829246ad
- Dalgard, C. L., Cole, J. T., Kean, W. S., Lucky, J. J., Sukumar, G., McMullen, D. C., et al. (2012). The cytokine temporal profile in rat cortex after controlled cortical impact. *Front. Mol. Neurosci.* 5:6. doi: 10.3389/fnmol.2012.00006

DATA AVAILABILITY STATEMENT

All data used during the current study are available from the corresponding author on reasonable request.

ETHICS STATEMENT

The animal study was reviewed and approved by the Experimental Animal Center of Nantong University (permission number: 20191106-003). Written informed consent was obtained from the owners for the participation of their animals in this study.

AUTHOR CONTRIBUTIONS

HH, AX, SL, CL, YL, LS, ZZ, and SW performed the experiments. SL conceived and designed the study. JC and XZ analyzed the data. All authors read and approved the final manuscript.

FUNDING

This project was funded by the National Natural Science Foundation of China (No. 81702223) and Science and Technology Planning Project of Nantong (MS22019006).

ACKNOWLEDGMENTS

We thank the staff members of our team for their cooperation in this work.

- Dou, Y., Tian, X., Zhang, J., Wang, Z., and Chen, G. (2018). Roles of traf6 in central nervous system. *Curr. Neuropharmacol.* 16, 1306–1313. doi: 10.2174/1570159X16666180412094655
- Gao, Y. J., Zhang, L., Samad, O. A., Suter, M. R., Yasuhiko, K., Xu, Z. Z., et al. (2009). Jnk-induced mcp-1 production in spinal cord astrocytes contributes to central sensitization and neuropathic pain. *J. Neurosci.* 29, 4096–4108. doi: 10.1523/JNEUROSCI.3623-08.2009
- Geng, F., Ma, Y., Xing, T., Zhuang, X., Zhu, J., and Yao, L. (2016). Effects of hyperbaric oxygen therapy on inflammasome signaling after traumatic brain injury. *Neuroimmunomodulation* 23, 122–129. doi: 10.1159/000445689
- Gyoneva, S., and Ransohoff, R. M. (2015). Inflammatory reaction after traumatic brain injury: therapeutic potential of targeting cell-cell communication by chemokines. *Trends Pharmacol. Sci.* 36, 471–480. doi: 10.1016/j.tips.2015.04.003
- Karve, I. P., Taylor, J. M., and Crack, P. J. (2016). The contribution of astrocytes and microglia to traumatic brain injury. *Br. J. Pharmacol.* 173, 692–702. doi: 10.1111/bph.13125
- Kim, J. Y., Lee, Y. W., Kim, J. H., Lee, W. T., Park, K. A., and Lee, J. E. (2015). Agmatine attenuates brain edema and apoptotic cell death after traumatic brain injury. *J. Korean Med. Sci.* 30, 943–952. doi: 10.3346/jkms.2015.30.7.943
- Kong, L., Yao, Y., Xia, Y., Liang, X., Ni, Y., and Yang, J. (2019). Osthole alleviates inflammation by down-regulating nf-kappab signaling pathway in traumatic brain injury. *Immunopharmacol. Immunotoxicol.* 41, 349–360. doi: 10.1080/08923973.2019.1608560

- Li, M., Zhang, D., Ge, X., Zhu, X., Zhou, Y., Zhang, Y., et al. (2019). Traf6-p38/jnk-atf2 axis promotes microglial inflammatory activation. *Exp. Cell Res.* 376, 133–148. doi: 10.1016/j.yexcr.2019.02.005
- Li, T., Qin, J. J., Yang, X., Ji, Y. X., Guo, F., Cheng, W. L., et al. (2017). The ubiquitin e3 ligase traf6 exacerbates ischemic stroke by ubiquitinating and activating racl1. *J. Neurosci.* 37, 12123–12140. doi: 10.1523/JNEUROSCI.1751-17.2017
- Liu, G. J., Zhang, Q. R., Gao, X., Wang, H., Tao, T., Gao, Y. Y., et al. (2020). Mir-146a ameliorates hemoglobin-induced microglial inflammatory response via tlr4/irak1/traf6 associated pathways. *Front. Neurosci.* 14:311. doi: 10.3389/fnins.2020.00311
- Liu, J., Xiong, X., and Sui, Y. (2019). Isoliquiritigenin attenuates neuroinflammation in traumatic brain injury in young rats. *Neuroimmunomodulation* 26, 102–110. doi: 10.1159/000495467
- Liu, S., Lu, C., Liu, Y., Zhou, X., Sun, L., Gu, Q., et al. (2018). Hyperbaric oxygen alleviates the inflammatory response induced by lps through inhibition of nf-kappab/mapks-ccl2/cxcl1 signaling pathway in cultured astrocytes. *Inflammation* 41, 2003–2011. doi: 10.1007/s10753-018-0843-2
- Liu, S., Shen, G., Deng, S., Wang, X., Wu, Q., and Guo, A. (2013a). Hyperbaric oxygen therapy improves cognitive functioning after brain injury. *Neural Regen. Res.* 8, 3334–3343. doi: 10.3969/j.issn.1673-5374.2013.35.008
- Liu, S., Zhang, L., Wu, Q., Wu, Q., and Wang, T. (2013b). Chemokine ccl2 induces apoptosis in cortex following traumatic brain injury. *J. Mol. Neurosci.* 51, 1021–1029. doi: 10.1007/s12031-013-0091-8
- Lu, Y., Jiang, B. C., Cao, D. L., Zhang, Z. J., Zhang, X., Ji, R. R., et al. (2014). Traf6 upregulation in spinal astrocytes maintains neuropathic pain by integrating tnf-alpha and il-1beta signaling. *Pain* 155, 2618–2629. doi: 10.1016/j.pain.2014.09.027
- Marshall, J., Szymdynger-Chodobska, J., Rioult-Pedotti, M. S., Lau, K., Chin, A. T., Kotla, S. K. R., et al. (2017). Trkb-enhancer facilitates functional recovery after traumatic brain injury. *Sci. Rep.* 7:10995. doi: 10.1038/s41598-017-11316-8
- Meng, X. E., Zhang, Y., Li, N., Fan, D. F., Yang, C., Li, H., et al. (2016). Hyperbaric oxygen alleviates secondary brain injury after trauma through inhibition of tlr4/nf-kappab signaling pathway. *Med. Sci. Monit.* 22, 284–288. doi: 10.12659/msm.894148
- Meng, Z., Zhao, T., Zhou, K., Zhong, Q., Wang, Y., Xiong, X., et al. (2017). A20 ameliorates intracerebral hemorrhage-induced inflammatory injury by regulating traf6 polyubiquitination. *J. Immunol.* 198, 820–831. doi: 10.4049/jimmunol.1600334
- Qian, H., Li, Q., and Shi, W. (2017). Hyperbaric oxygen alleviates the activation of nlrp3 inflammasomes in traumatic brain injury. *Mol. Med. Rep.* 16, 3922–3928. doi: 10.3892/mmr.2017.7079
- Semple, B. D., Bye, N., Rancan, M., Ziebell, J. M., and Morganti-Kossmann, M. C. (2010). Role of ccl2 (mcp-1) in traumatic brain injury (tbi): evidence from severe tbi patients and ccl2^{-/-} mice. *J. Cereb. Blood Flow Metab.* 30, 769–782. doi: 10.1038/jcbfm.2009.262
- Simon, D. W., Mcgeachy, M. J., Bayir, H., Clark, R. S. B., Loane, D. J., and Kochanek, P. M. (2017). The far-reaching scope of neuroinflammation after traumatic brain injury. *Nat. Rev. Neurol.* 13, 171–191. doi: 10.1038/nrneuro.2017.13
- Song, F., Zeng, K., Liao, L., Yu, Q., Tu, P., and Wang, X. (2016). Schizandrin a inhibits microglia-mediated neuroninflammation through inhibiting traf6-nf-kappab and jak2-stat3 signaling pathways. *PLoS One* 11:e0149991. doi: 10.1371/journal.pone.0149991
- Tucker, L. B., Velosky, A. G., and McCabe, J. T. (2018). Applications of the morris water maze in translational traumatic brain injury research. *Neurosci. Biobehav. Rev.* 88, 187–200. doi: 10.1016/j.neubiorev.2018.03.010
- Wan, S. Y., Li, G. S., Tu, C., Chen, W. L., Wang, X. W., Wang, Y. N., et al. (2021). Micronar-194-5p hinders the activation of nlrp3 inflammasomes and alleviates neuroinflammation during intracerebral hemorrhage by blocking the interaction between traf6 and nlrp3. *Brain Res.* 1752:147228. doi: 10.1016/j.brainres.2020.147228
- Webster, K. M., Sun, M., Crack, P., O'Brien, T. J., Shultz, S. R., and Semple, B. D. (2017). Inflammation in epileptogenesis after traumatic brain injury. *J. Neuroinflammation* 14:10. doi: 10.1186/s12974-016-0786-1
- Wu, G., McBride, D. W., and Zhang, J. H. (2018). Axl activation attenuates neuroinflammation by inhibiting the tlr/traf/nf-kappab pathway after mcao in rats. *Neurobiol. Dis.* 110, 59–67. doi: 10.1016/j.nbd.2017.11.009
- Xiong, Y., Mahmood, A., and Chopp, M. (2013). Animal models of traumatic brain injury. *Nat. Rev. Neurosci.* 14, 128–142. doi: 10.1038/nrn3407
- Yang, H., Gu, Z. T., Li, L., Maegele, M., Zhou, B. Y., Li, F., et al. (2017). Sirt1 plays a neuroprotective role in traumatic brain injury in rats via inhibiting the p38 mapk pathway. *Acta Pharmacol. Sin.* 38, 168–181. doi: 10.1038/aps.2016.130
- Zeng, K. W., Yu, Q., Liao, L. X., Song, F. J., Lv, H. N., Jiang, Y., et al. (2015). Anti-neuroinflammatory effect of mc13, a novel coumarin compound from condiment murraya, through inhibiting lipopolysaccharide-induced traf6-tak1-nf-kappab, p38/erk mapks and jak2-stat1/stat3 pathways. *J. Cell. Biochem.* 116, 1286–1299. doi: 10.1002/jcb.25084

Conflict of Interest: The authors declare that the research was conducted in the absence of any commercial or financial relationships that could be construed as a potential conflict of interest.

Copyright © 2021 Huang, Xia, Sun, Lu, Liu, Zhu, Wang, Cai, Zhou and Liu. This is an open-access article distributed under the terms of the Creative Commons Attribution License (CC BY). The use, distribution or reproduction in other forums is permitted, provided the original author(s) and the copyright owner(s) are credited and that the original publication in this journal is cited, in accordance with accepted academic practice. No use, distribution or reproduction is permitted which does not comply with these terms.